MASTER COPY: PLEASE KEEP THIS "MEMORANDUM OF TRANSMITTAL" BLANK FOR REPRODUCTION PURPOSES. WHEN REPORTS ARE GENERATED UNDER THE ARO SPONSORSHIP, FORWARD A COMPLETED COPY OF THIS FORM WITH EACH REPORT SHIPMENT TO THE ARO. THIS WILL ASSURE PROPER IDENTIFICATION. NOT TO BE USED FOR INTERIM PROGRESS REPORTS; SEE PAGE 2 FOR INTERIM PROGRESS REPORT INSTRUCTIONS.

MEMORANDUM OF TRANSMITTAL

U.S. Army Research Office
ATTN: AMSRL-RO-BI (TR)
P.O. Box 12211
Research Triangle Park, NC 27709-2211

- [x] Reprint (Orig + 2 copies)
- [ ] Manuscript (1 copy)
- [ ] Technical Report (Orig + 2 copies)
- [ ] Final Progress Report (Orig + 2 copies)
- [ ] Related Materials, Abstracts, Theses (1 copy)

CONTRACT/GRANT NUMBER: W911NF-04-1-0244 (46637-CI-MUR)

REPORT TITLE: Demodulation and Performance Analysis of Differential Unitary Space-Time Modulation in Time-Varying Rician Channels

is forwarded for your information.

SUBMITTED FOR PUBLICATION TO (applicable only if report is manuscript):

PUPLISHED BY: Proceedings of the 64th IEEE Vehicular Technology Conference
Montreal, Canada, 25-28 September 2006

Sincerely,

Dr. James Zeidler
Department of Electrical and Computer Engineering
University of California, San Diego

REPORT DOCUMENTATION PAGE

Form Approved
OMB NO. 0704-0188

1. AGENCY USE ONLY (Leave Blank)	2. REPORT DATE	3. REPORT TYPE AND DATES COVERED
	08/21/2006	**Manuscripts: 01 Jan. 2006 - 31 Dec 2006**

4. TITLE AND SUBTITLE

Demodulation and Performance Analysis of Differential Unitary Space-Time Modulation in Time-Varying Rician Channels

5. FUNDING NUMBERS

W911NF0410224

6. AUTHOR(S)

Haichang Sui, James R. Zeidler

7. PERFORMING ORGANIZATION NAME(S) AND ADDRESS(ES)

University of California - San Diego
Office of Contract & Grant Administration
9500 Gilman Dr. Mail Code 0934, La Jolla, CA, 92093-0934

8. PERFORMING ORGANIZATION REPORT NUMBER

9. SPONSORING / MONITORING AGENCY NAME(S) AND ADDRESS(ES)

U. S. Army Research Office
P.O. Box 12211
Research Triangle Park, NC 27709-2211

10. SPONSORING / MONITORING AGENCY REPORT NUMBER

11. SUPPLEMENTARY NOTES

The views, opinions and/or findings contained in this report are those of the author(s) and should not be construed as an official Department of the Army position, policy or decision, unless so designated by other documentation.

12 a. DISTRIBUTION / AVAILABILITY STATEMENT	12 b. DISTRIBUTION CODE
Approved for public release; distribution unlimited.	**N/A**

13. ABSTRACT (Maximum 200 words)

Studies on differential unitary space-time modulation are mostly focused on Rayleigh fading channels. In this paper we present new analytic results for the maximum-likelihood demodulator (MLD) and the standard differential demodulator (SDD). The resulting expressions and bounds on the pairwise error probability shed light on the impact of various system parameters and are helpful towards a deeper understanding of the DUSTM in Rician channels. Additional analytic results are also derived for the constellation in [3]. Unlike in Rayleigh fading, the exact MLD can only be implemented approximately [8]. The performance loss of practical demodulator such as the SDD and a prediction-based demodulator relative to the MLD are studied under different Rician fading environments.

14. SUBJECT TERMS	15. NUMBER OF PAGES
N/A	**5**
	16. PRICE CODE **N/A**

17. SECURITY CLASSIFICATION OR REPORT	18. SECURITY CLASSIFICATION ON THIS PAGE	19. SECURITY CLASSIFICATION OF ABSTRACT	20. LIMITATION OF ABSTRACT
UNCLASSIFIED	**UNCLASSIFIED**	**UNCLASSIFIED**	**UL**

NSN 7540-01-280-5500

Standard Form 298 (Rev.2-89)
Prescribed by ANSI Std. 239-18
298-102

Enclosure 1

Demodulation and Performance Analysis of Differential Unitary Space-Time Modulation in Time-Varying Rician Channels

Haichang Sui and James R. Zeidler
Dept. of Electrical & Computer Engineering, Univ. of California, San Diego, La Jolla, CA 92093-0407
Emails: hsui@ucsd.edu, zeidler@ece.ucsd.edu

***Abstract*— Studies on differential unitary space-time modulation are mostly focused on Rayleigh fading channels. In this paper we present new analytic results for the maximum-likelihood demodulator (MLD) and the standard differential demodulator (SDD). The resulting expressions and bounds on the pairwise error probability shed light on the impact of various system parameters and are helpful towards a deeper understanding of the DUSTM in Rician channels. Additional analytic results are also derived for the constellation in [3]. Unlike in Rayleigh fading, the exact MLD can only be implemented approximately [8]. The performance loss of practical demodulator such as the SDD and a prediction-based demodulator relative to the MLD are studied under different Rician fading environments.**

Keywords: differential, space-time, Rician channel, maximum-likelihood, pairwise error probability, performance analysis

I. Introduction

Differential unitary space-time modulation (DUSTM) is proposed in [1] as an effective transmission scheme in fast-fading environment. Previous studies are mostly focused on Rayleigh fading channels (e.g. [9] and references therein), while analytic results for DUSTM under Rician channels are relatively scarce. The performance of the standard differential demodulator (SDD) as in [1] is analyzed in [5] [6] where the Rician channel consists of a time-invariant line-of-sight (LOS) component and a diffuse component obeying a first-order AR model. Lampe and Schober [7] consider a prediction based demodulator (PBD) under a more general Rician channel model whose LOS component is time-varying and the diffuse component can have arbitrary time-correlation. Although it offers improved performance over the SDD, the PBD in [7] is not necessarily optimum in the maximum-likelihood sense.

In this paper, the maximum-likelihood demodulator (MLD) based on two received space-time blocks as with the SDD is derived. Unlike the SDD or the PBD, the transmitted signal in the previous block is involved in the MLD for the symbol transmitted in the current block. Thus, the exact MLD can only be implemented approximately [8], but its performance can be viewed as a bound on all other demodulators based on the same received data. Furthermore, while the SDD and the one-tap PBD are shown to be equivalent to the MLD in Rayleigh fading under certain assumptions [4] [9], such an equivalence does not follow in the Rician fading. The performance of the SDD, PBD, and MLD are compared under different environments in this paper. Significant gaps are observed when the line-of-sight (LOS) component in the channel is either strong or fast time-varying.

In contrast to the Rayleigh fading case, insightful performance analysis for DUSTM in Rician channels is not found in the literature. In this paper, we present new expressions and bounds of the pairwise error probability (PEP) for the MLD and the SDD. The resulting PEP is expressed by an infinite sum where the summands are finite integrals depending on the effective SNR, the constellation property, and the fading statistics. An insightful bound is also obtained on the PEP, from which the impact of different system parameters can be better understood. Furthermore, for the specific constellation in [3], we obtain the PEP without involving integrations.

As we will see later, the PEP analysis is related to the distribution of a quadratic form of Gaussian vectors. Alternative analytic expressions for the PEP may be obtained by applying the results for general quadratic forms of Gaussian vectors [10]-[13]. However, insight is not easily obtained by applying those general results because they do not explicitly utilize the specific structures of the unitary matrices in the DUSTM constellation, the covariance matrix of the received signals, and the Hermitian matrix in the quadratic form. In contrast, our results are directly related to physically meaningful metrics such as the effective SNR, the diversity product of the constellation [1], and the Rician statistics. Furthermore, the results in [11] [12] [13] may be hard to evaluate in practice, since they require either an infinite sum with recursive computation for higher derivatives of certain functions [12] or involves doubly infinite summations [11] [13]. The PEP expression obtained here involves a single infinite sum and finite integrals without requiring recursive computation of higher derivatives. For the specific constellation in [3], we further obtain the PEP without integrations. Consequently, our results may have computational advantage over the results in [11] [12] [13].

The rest of the paper is organized as follows. The system model is presented in Section II. The likelihood function and the MLD is derived in Section III. The PEP of the MLD

This work is supported by, or in part by, the U. S. Army Research Office under the Multi-University Research Initiative (MURI) grant # W911NF-04-1-0224, the Office of Naval Research (Code 313), and the UCSD Center for Wireless Communications (UC IUCRP grant #03-10148).

and the SDD is analyzed in Section IV for general DUSTM constellations while results specific to the constellations proposed in [3] are presented in Section V. Section VI contains numerical results and Section VII concludes the paper.

Throughout the paper, we use the notation $\overline{\mathbf{X}}$ to denote the mean of a random matrix $\mathbf{X}$ and denote $\widetilde{\mathbf{X}} = \mathbf{X} - \overline{\mathbf{X}}$. When the columns of $\mathbf{X}$ are i.i.d. circularly symmetric complex Gaussian vectors, the distribution of $\mathbf{X}$ is denoted as $\mathbf{X} \overset{c.i.}{\sim} \mathcal{CN}\left(\overline{\mathbf{X}}, \mathbf{C}\right)$, where $\mathbf{C}$ is the covariance matrix of any column of $\mathbf{X}$. The Frobenius norm and the determinant of a matrix are denoted by $\|\cdot\|_F$ and $|\cdot|$, respectively. The CF of a r.v. X is defined as $\phi(s) = \mathrm{E}\left[e^{-sX}\right]$.

II. System Model

The transmitter model is the same as in [1] and [9]. The transmission is partitioned into blocks of time duration T_s. Within $[\tau T_s, (\tau+1)T_s]$, an $M \times M$ space-time matrix $\mathbf{S}_\tau = \mathbf{V}_{z_\tau} \mathbf{S}_{\tau-1}$ ($z_\tau = 0, \ldots, L{-}1$) is transmitted from the M antennas in M consecutive channel uses. Without loss of generality, we set the initial transmission $\mathbf{S}_0 = \mathbf{I}_M$. The set of all possible $\mathbf{S}_\tau$ is denoted as $\mathcal{S}$, which is identical to $\mathcal{V} = \{\mathbf{V}_0, \ldots, \mathbf{V}_{L-1}\}$ only if $\mathcal{V}$ forms a group under matrix multiplication.

The channel is assumed to be frequency-flat and time-invariant in each T_s block. For N receive antennas, the equivalent discrete channel in $[\tau T_s, (\tau+1)T_s]$ is represented by an $M \times N$ matrix $\mathbf{H}_\tau$ whose $(i,j)^{\text{th}}$ entry, $h_{i,j,\tau}$, is the fading coefficient between the i^{th} transmit antenna and the j^{th} receive antenna. Thus, the received space-time signal in $[\tau T_s, (\tau+1)T_s]$ together with AWGN can be written as

$$\mathbf{R}_\tau = \mathbf{S}_\tau \mathbf{H}_\tau + \mathbf{W}_\tau \tag{1}$$

where $\mathbf{W}_\tau \overset{c.i.}{\sim} \mathcal{CN}\left(\mathbf{0}, \sigma_w^2 \mathbf{I}_M\right)$ and each column of $\mathbf{R}_\tau$ consists of symbols received on the corresponding antenna.

Rician fading is considered in this paper. That is, the channel coefficient $h_{i,j,\tau}$ is distributed as $\mathcal{CN}\left(\overline{h}_{i,j,\tau}, \sigma_h^2\right)$. The processes $\{\tilde{h}_{i,j,\tau}\}_\tau$ for different (i,j) pairs are assumed to be uncorrelated and have the same normalized covariance coefficients $\varphi_{h,\xi} = \mathrm{E}\{\tilde{h}_{i,j,\tau+\xi} \tilde{h}^*_{i,j,\tau}\}/\sigma_h^2$. The time-varying LOS component $\overline{h}_{i,j,\tau}$ is modelled as $\overline{h}_{i,j,\tau} = e^{j2\pi f_L T_s \tau} \mu_{i,j}$ where f_L is the Doppler shift of the LOS component and $\mu_{i,j} \in \mathbb{C}$ does not depend on τ. This allows the receive antennas to have different phase responses to the LOS signal. We assume $|\mu_{i,j}|$ to be independent of i or j and, without loss of generality, normalize the channel gains such that $\mathrm{E}\{|h_{i,j,\tau}|^2\} = |\mu_{i,j}|^2 + \sigma_h^2 = 1$. Consequently, the received SNR on each antenna is $\rho = 1/\sigma_w^2$ since $\mathbf{S}_\tau$ is unitary. Furthermore, by defining the Rician factor to be $K \triangleq |\mu_{i,j}|^2/\sigma_h^2$, it is easy to see that $|\mu_{i,j}|^2 = \frac{K}{K+1}$ and $\sigma_h^2 = \frac{1}{K+1}$.

III. Demodulation Schemes

We consider the demodulation of z_τ from the received signal $\mathbf{R}_{\tau-1}$ and $\mathbf{R}_\tau$. Conditioning on $\mathbf{S}_{\tau-1}$ and $z_\tau = l$, the concatenated vector $\mathbf{R}_\tau^{\tau-1} \triangleq \left[\mathbf{R}_{\tau-1}^H, \mathbf{R}_\tau^H\right]^H$ is distributed as $\mathbf{R}_\tau^{\tau-1} \overset{c.i.}{\sim} \mathcal{CN}\left(\overline{\mathbf{R}}_\tau^{\tau-1}, \mathbf{C}_l\right)$ where

$$\overline{\mathbf{R}}_\tau^{\tau-1} = \begin{bmatrix} \mathbf{S}_{\tau-1}\overline{\mathbf{H}}_{\tau-1} \\ \mathbf{V}_l \mathbf{S}_{\tau-1} \overline{\mathbf{H}}_\tau \end{bmatrix}, \; \mathbf{C}_l = \begin{bmatrix} \left(\sigma_h^2 + \sigma_w^2\right)\mathbf{I}_M & \varphi_{h,1}^* \sigma_h^2 \mathbf{V}_l^H \\ \varphi_{h,1}\sigma_h^2 \mathbf{V}_l & \left(\sigma_h^2 + \sigma_w^2\right)\mathbf{I}_M \end{bmatrix}. \tag{2}$$

Consequently, the likelihood function can be written as

$$f\left(\mathbf{R}_\tau^{\tau-1} | l\right) = \frac{\exp\left\{-\operatorname{tr}\left[\left(\widetilde{\mathbf{R}}_\tau^{\tau-1}\right)^H \mathbf{C}_l^{-1} \widetilde{\mathbf{R}}_\tau^{\tau-1}\right]\right\}}{\pi^{2MN} |\mathbf{C}_l|^N}. \tag{3}$$

It can be shown that $|\mathbf{C}_l|$ does not depend on $\mathbf{S}_{\tau-1}$ or l [9]. By incorporating (2) and after some algebra, the exponent in (3) reduces to

$$-\operatorname{tr}\left[\left(\widetilde{\mathbf{R}}_\tau^{\tau-1}\right)^H \mathbf{C}_l^{-1} \widetilde{\mathbf{R}}_\tau^{\tau-1}\right] = c_1 + \frac{c_2}{2} \cdot \left\|\mathbf{U}_\tau + \mathbf{V}_l^H \mathbf{R}_\tau\right\|_F^2 \tag{4}$$

where

$$\mathbf{U}_\tau \triangleq \frac{\varphi_{h,1}}{|\varphi_{h,1}|}\widetilde{\mathbf{R}}_{\tau-1} + \frac{1 + \sigma_w^2/\sigma_h^2}{|\varphi_{h,1}|}\mathbf{S}_{\tau-1}\overline{\mathbf{H}}_\tau \;, \tag{5}$$

and c_1, c_2 are constants independent of l. Thus, the MLD is

$$(\hat{z}_\tau)_{\text{MLD}} = \arg\max_l \left\|\mathbf{V}_l^H \mathbf{R}_\tau + \mathbf{U}_\tau\right\|_F^2 \quad . \tag{6}$$

Although (6) is optimal in the sense of minimizing the symbol error probability, exact MLD may not be implementable because $\mathbf{U}_\tau$ in (5) involves the space-time matrix transmitted in the $(\tau-1)^{\text{th}}$ block $\mathbf{S}_{\tau-1}$, which can only be estimated at the receiver [8]. On the other hand, the SDD originally proposed in [1] does not require such knowledge. The SDD heuristically uses $\mathbf{R}_{\tau-1}$ as a reference in demodulating z_τ by

$$(\hat{z}_\tau)_{\text{SDD}} = \arg\max_l \left\|\mathbf{V}_l^H \mathbf{R}_\tau + \mathbf{R}_{\tau-1}\right\|_F^2 \quad . \tag{7}$$

However, it is well-known that the SDD performs poorly when the variation between $\mathbf{H}_\tau$ and $\mathbf{H}_{\tau-1}$ are significant. To reduce the gap between the SDD and the MLD, the prediction based demodulator (PBD) proposed in [7] can be employed. Based on $\mathbf{R}_{\tau-1}$ and $\mathbf{R}_\tau$, the PBD in [7] is given by

$$(\hat{z}_\tau)_{\text{PBD}} = \arg\max_l \left\|\mathbf{V}_l^H \mathbf{R}_\tau + p\mathbf{R}_{\tau-1}\right\|_F^2 \quad . \tag{8}$$

where the one-tap prediction weight $p \in \mathbb{C}$ is chosen to minimize $\mathrm{E}\left\|p\mathbf{R}_{\tau-1} - \mathbf{S}_{\tau-1}\mathbf{H}_\tau\right\|_F^2$. This is motivated because we would intuitively prefer $p\mathbf{R}_{\tau-1}$ to be as close as possible to the equivalent channel $\mathbf{S}_{\tau-1}\mathbf{H}_\tau$ in $\mathbf{R}_\tau = \mathbf{V}_{z_\tau}(\mathbf{S}_{\tau-1}\mathbf{H}_\tau) + \mathbf{W}_\tau$. The weight p can be easily solve to be $p = \frac{Ke^{j2\pi f_L T_s} + \varphi_{h,1}}{(1+\sigma_w^2)(K+1)}$.

It is interesting to compare the MLD in Rician fading with its counterpart in Rayleigh fading. As shown in [4] [9], the MLD for Rayleigh fading is given by (6) with $\mathbf{U}_\tau = \frac{\varphi_{h,1}}{|\varphi_{h,1}|}\mathbf{R}_{\tau-1}$. In contrast, (5) can be rewritten as

$$\mathbf{U}_\tau = \frac{\left(1 + \sigma_w^2 + K\sigma_w^2\right) - e^{-j2\pi f_L T_s}\varphi_{h,1}}{|\varphi_{h,1}|}\mathbf{S}_{\tau-1}\overline{\mathbf{H}}_\tau + \frac{\varphi_{h,1}}{|\varphi_{h,1}|}\mathbf{R}_{\tau-1}. \tag{9}$$

In general, $\mathbf{U}_\tau \neq \frac{\varphi_{h,1}}{|\varphi_{h,1}|}\mathbf{R}_{\tau-1}$ for $K > 0$. At large K, $\mathbf{U}_\tau$ approximates the LOS channel $\overline{\mathbf{H}}_\tau$ after a trivial scaling that will not affect the performance. Consequently, unlike in the Rayleigh fading where the SDD and the one tap PBD are also MLD as long as $\varphi_{h,1} \in \mathbb{R}^+$, such an equivalence does not hold in Rician fading.

IV. Performance Analysis

A. Problem formulation

To facilitate the derivation, we denote

$$\mathbf{X}_\tau \triangleq \begin{bmatrix} \mathbf{U}_\tau \\ \mathbf{R}_\tau \end{bmatrix} \text{ and } \mathbf{\Phi}_l \triangleq \frac{1}{\sqrt{2}} \begin{bmatrix} \mathbf{I}_M \\ \mathbf{V}_l \end{bmatrix}. \tag{10}$$

The test statistics in (6) for hypothesis l is equivalent to $Z_l \triangleq \left\| \mathbf{\Phi}_l^H \mathbf{X}_\tau \right\|_F^2$. Since the PEP can be expressed as $P_e(k,l) = \Pr(Z_k - Z_l > 0 \mid l)$, it is equivalent to analyze $\Pr\left[\operatorname{tr}\left(\mathbf{X}_\tau^H \mathbf{Q} \mathbf{X}_\tau\right) > 0\right]$ where $\mathbf{X}_\tau \overset{c.i.}{\sim} \mathcal{CN}\left(\overline{\mathbf{X}}_\tau, \mathbf{C}_x\right)$ and $\mathbf{Q} = \mathbf{\Phi}_k \mathbf{\Phi}_k^H - \mathbf{\Phi}_l \mathbf{\Phi}_l^H$.

By setting $\mathbf{U}_\tau$ in (10) accordingly, different demodulators including the MLD (6), SDD (7), and PBD (8) can be obtained. The mean $\overline{\mathbf{X}}_\tau$ and the covariance matrix $\mathbf{C}_x$ depends on the choice of the demodulator. For example, it can be shown that

$$\overline{\mathbf{X}}_\tau = \begin{bmatrix} \frac{1+\sigma_w^2/\sigma_h^2}{|\varphi_{h,1}|} \mathbf{S}_{\tau-1} \overline{\mathbf{H}}_\tau \\ \mathbf{V}_l \mathbf{S}_{\tau-1} \overline{\mathbf{H}}_\tau \end{bmatrix}, \mathbf{C}_x = \begin{bmatrix} \left(\alpha + \frac{|\beta|}{2}\right)\mathbf{I}_M & \frac{|\beta|}{2}\mathbf{V}_l^H \\ \frac{|\beta|}{2}\mathbf{V}_l & \left(\alpha + \frac{|\beta|}{2}\right)\mathbf{I}_M \end{bmatrix} \tag{11}$$

when the MLD is considered, while for the SDD we have

$$\overline{\mathbf{X}}_\tau = \begin{bmatrix} \mathbf{S}_{\tau-1} \overline{\mathbf{H}}_{\tau-1} \\ \mathbf{V}_l \mathbf{S}_{\tau-1} \overline{\mathbf{H}}_\tau \end{bmatrix}, \mathbf{C}_x = \begin{bmatrix} \left(\alpha + \frac{|\beta|}{2}\right)\mathbf{I}_M & \frac{\beta^*}{2}\mathbf{V}_l^H \\ \frac{\beta}{2}\mathbf{V}_l & \left(\alpha + \frac{|\beta|}{2}\right)\mathbf{I}_M \end{bmatrix} \tag{12}$$

where $\beta \triangleq 2\varphi_{h,1}\sigma_h^2$ and $\alpha \triangleq \sigma_h^2\left(1 - |\varphi_{h,1}|\right) + \sigma_w^2$. In the following, we analyze the PEP for the MLD, which is a bound for all practical demodulators based on $\mathbf{R}_{\tau-1}$ and $\mathbf{R}_\tau$. However, by noticing the similarity between $\mathbf{C}_x$ in (11) and (12), the analysis applies equally for the SDD when $\varphi_{h,1} \in \mathbb{R}^+$ and the performance of the SDD can be obtained by substituting $\overline{\mathbf{X}}_\tau$ from (12) into the results to follow. The condition $\varphi_{h,1} \in \mathbb{R}^+$ is usually satisfied in commonly used channel models. For example, $\varphi_{h,1}$ equals $J_0(2\pi f_D T_s)$ in the Jakes' model and is positive for a wide range of normalized Doppler shifts $f_D T_s$ for the diffuse fading component.

B. Characteristic Function

If we denote the SVD of $\mathbf{\Phi}_k^H \mathbf{\Phi}_l$ by $\mathbf{\Theta}\mathbf{D}\mathbf{\Upsilon}^H$ and define

$$\mathbf{Y} \triangleq \begin{bmatrix} \mathbf{Y}_1 \\ \mathbf{Y}_2 \end{bmatrix} \triangleq \sqrt{\frac{|\beta|}{\alpha + |\beta|}} \begin{bmatrix} \mathbf{\Upsilon}^H \mathbf{\Phi}_l^H \mathbf{X}_\tau \\ \mathbf{\Theta}^H \mathbf{\Phi}_k^H \mathbf{X}_\tau \end{bmatrix},$$

we have the following decomposition

$$\frac{|\beta|}{\alpha + |\beta|} \mathbf{X}_\tau^H \mathbf{Q} \mathbf{X}_\tau = \sum_{n=1}^{N} \sum_{m=1}^{M} \left(|y_{2,m,n}|^2 - |y_{1,m,n}|^2 \right) \tag{13}$$

where $y_{1,m,n}$ and $y_{2,m,n}$ are the $(m,n)^{\text{th}}$ elements of $\mathbf{Y}_1$ and $\mathbf{Y}_2$ respectively. The factor $\frac{|\beta|}{\alpha+|\beta|}$ in (13) will not affect the PEP analysis. From $\mathbf{X}_\tau \overset{c.i.}{\sim} \mathcal{CN}\left(\overline{\mathbf{X}}_\tau, \mathbf{C}_x\right)$, we conclude that $\mathbf{Y} \overset{c.i.}{\sim} \mathcal{CN}\left(\overline{\mathbf{Y}}, \mathbf{C}_y\right)$ where

$$\overline{\mathbf{Y}} \triangleq \begin{bmatrix} \overline{\mathbf{Y}}_1 \\ \overline{\mathbf{Y}}_2 \end{bmatrix} = \sqrt{\frac{|\beta|}{2(\alpha + |\beta|)}} \begin{bmatrix} \mathbf{\Upsilon}^H \mathbf{\Phi}_l^H \overline{\mathbf{X}}_\tau \\ \mathbf{\Theta}^H \mathbf{\Phi}_k^H \overline{\mathbf{X}}_\tau \end{bmatrix}. \tag{14}$$

The diagonal matrix $\mathbf{D} = \operatorname{diag}(d_1, \ldots, d_M)$ contains the singular values of $\mathbf{\Phi}_k^H \mathbf{\Phi}_l$ and $1 - d_m^2 = \sigma_m^2/4$, where σ_m is the m^{th} singular value of $\mathbf{V}_k - \mathbf{V}_l$. Without loss of generality, we can assume $1 \geq d_1 \geq \ldots \geq d_M \geq 0$. By noticing $\mathbf{C}_x$ in (11) equals to $|\beta| \mathbf{\Phi}_l \mathbf{\Phi}_l^H + \alpha \mathbf{I}_{2M}$, the matrix $\mathbf{C}_y$ can be simplified to

$$\mathbf{C}_y = |\beta| \begin{bmatrix} \mathbf{I}_M & \mathbf{D} \\ \mathbf{D} & \frac{1}{\alpha+|\beta|}\left(|\beta| \mathbf{D}^2 + \alpha \mathbf{I}_M\right) \end{bmatrix}. \tag{15}$$

The structure of $\mathbf{C}_y$ implies that (13) can be viewed as a sum of MN independent r.v.s, each of which is expressed as a quadratic form $\mathbf{y}_{m,n}^H \mathbf{Q}_2 \mathbf{y}_{m,n}$where $\mathbf{y}_{m,n} \triangleq [y_{1,m,n}, y_{2,m,n}]^T$ and $\mathbf{Q}_2 = \operatorname{diag}(-1, 1)$. The CF for $\mathbf{y}_{m,n}^H \mathbf{Q}_2 \mathbf{y}_{m,n}$ is readily available from the results in [10]. The CF of either side of (13) is the product of the CFs for all $\mathbf{y}_{m,n}^H \mathbf{Q}_2 \mathbf{y}_{m,n}$ ($m = 1, \ldots, M$, $n = 1, \ldots, N$) and can be shown to be

$$\phi(s) = e^{-f_1} \sum_{n=0}^{\infty} \frac{1}{n!} \frac{G^n(s)}{D^{N+n}(s)} \tag{16}$$

where $D(s)$, $G(s)$, and $f_1 \triangleq \sum_{m=1}^{M} \sum_{n=1}^{N} f_{1,m,n}$ are given by

$$D(s) = \prod_{m=1}^{M} b_m^2 \left[a_m^2 - \left(s + \frac{1}{2\alpha}\right)^2 \right], \tag{17}$$

$$G(s) = \sum_{m=1}^{M} \left(\sum_{n=1}^{N} f_{1,m,n} + s \sum_{n=1}^{N} f_{2,m,n} \right) \prod_{\substack{i=1 \\ i \neq m}}^{M} D_m(s), \tag{18}$$

$$b_m = \sqrt{\frac{\alpha |\beta|^2 \sigma_m^2}{4(\alpha + |\beta|)}}, \quad a_m = \sqrt{\frac{1}{4\alpha^2} + b_m^{-2}}, \tag{19}$$

$$f_{1,m,n} = \frac{\alpha + |\beta|}{\alpha |\beta| (1 - d_m^2)} \Big[\frac{\alpha + |\beta| d_m^2}{\alpha + |\beta|} |\overline{y}_{1,m,n}|^2 + |\overline{y}_{2,m,n}|^2 - 2 d_m \operatorname{Re}\left(\overline{y}_{1,m,n} \overline{y}_{2,m,n}^*\right) \Big] \tag{20}$$

$$f_{2,m,n} = \frac{1}{\alpha} \Big[\frac{\left(\alpha^2 - |\beta|^2 d_m^2\right)}{\alpha + |\beta|} |\overline{y}_{1,m,n}|^2 - (\alpha + |\beta|) |\overline{y}_{2,m,n}|^2 + 2|\beta| d_m \operatorname{Re}\left(\overline{y}_{1,m,n} \overline{y}_{2,m,n}^*\right) \Big]$$

C. Pairwise Error Probability

The PEP can be obtained as

$$P_e(k,l) = \frac{1}{2\pi i} \int_0^\infty dx \int_{\mathcal{C}} \phi(s) e^{sx} ds. \tag{21}$$

From (17), we know that the ROC of $\phi(s)$ is $-\frac{1}{2\alpha} - a_m < \operatorname{Re}(s) < -\frac{1}{2\alpha} + a_m$. Therefore, we can choose the integral contour to be $\mathcal{C} = \left\{ \operatorname{Re}(s) = -\frac{1}{2\alpha} \right\}$. This also justifies swap of integrals in (21). After substituting (16) into (21), changing the variable $s=-\frac{1}{2\alpha}+i\frac{\tan\theta}{2\alpha}$, and taking the real part, we obtain

$$P_e(k,l) = \frac{\alpha e^{-f_1}}{\pi}\sum_{n=0}^{\infty}\frac{1}{n!}\int_{-\pi/2}^{\pi/2}\widetilde{G}_n(\theta) \times\prod_{m=1}^{M}\left[1+\frac{\overline{\rho}}{4\cos^2\theta}\sigma_m^2\right]^{-(N+n)}d\theta \quad (22)$$

where

$$\widetilde{G}_n(\theta) \triangleq \frac{1}{2\alpha}\mathrm{Re}\left[G^n\left(-\frac{1}{2\alpha}+i\frac{\tan\theta}{2\alpha}\right)\right] -\frac{\tan\theta}{2\alpha}\cdot\mathrm{Im}\left[G^n\left(-\frac{1}{2\alpha}+i\frac{\tan\theta}{2\alpha}\right)\right]$$

and $\overline{\rho}$ is the effective SNR through the diffuse fading component, which is defined by

$$\overline{\rho}\triangleq\frac{|\beta|^2}{4\alpha(\alpha+|\beta|)}=\frac{|\varphi_{h,1}|^2\left(\frac{\rho}{K+1}\right)^2}{\left(1-|\varphi_{h,1}|^2\right)\left(\frac{\rho}{K+1}\right)^2+2\frac{\rho}{K+1}+1}. \quad (23)$$

Equation (23) is the same as the effective SNR for Rayleigh fading in [9] except now the SNR per receive antenna through the diffuse fading component is $\frac{\rho}{K+1}$.

The PEP in (22) can be bounded by

$$P_e(k,l) \leq \frac{\alpha e^{-f_1}}{\pi}\sum_{n=0}^{\infty}\frac{1}{n!}\int_{-\pi/2}^{\pi/2}\left|\widetilde{G}_n(\theta)\right| \times\prod_{m=1}^{M}\left[1+\frac{\overline{\rho}}{4\cos^2\theta}\sigma_m^2\right]^{-(N+n)}d\theta \quad (24)$$

As proved in [1], a DUSTM constellation achieves full diversity if $\prod_{m=1}^{M}\sigma_m^2$ or equivalently $|\mathbf{V}_k-\mathbf{V}_l|$ not equal to 0. If we assume this is true for all distinct $\mathbf{V}_k,\mathbf{V}_l$ in the $\mathcal{V}$ under consideration, (24) can be further bounded by

$$P_e(k,l) \leq \frac{\alpha e^{-f_1}}{\pi}\left(\frac{\overline{\rho}}{4}\right)^{-MN}|\mathbf{V}_k-\mathbf{V}_l|^{-2N}\sum_{n=0}^{\infty}\left(\frac{\overline{\rho}}{4}\right)^{-nM} \frac{|\mathbf{V}_k-\mathbf{V}_l|^{-2n}}{n!}\int_{-\pi/2}^{\pi/2}|\widetilde{G}_n(\theta)|\left(\cos\theta\right)^{2M(N+n)}d\theta \quad (25)$$

Although the bound in (25) involves an infinite sum and cannot be expressed in closed-form, it is not available in the literature and sheds light on the performance of DUSTM under the Rician fading model. For example, we observe that the effect of the LOS fading component is encapsulated in $\widetilde{G}_n(\theta)$ only; the time-variation of the diffuse fading component and the SNR is captured in the effective SNR $\overline{\rho}$; and the properties of the constellation reflects in $|\mathbf{V}_k-\mathbf{V}_l|$, which is also related to the so-called diversity product [1].

V. Results for a Special Constellation

The results derived in the previous section apply for general DUSTM constellations. Although the analysis shed some light on the performance, the integrals in (22) and (25) have to be computed by numerical methods. In this section, we focus on a class of 2×2 constellations proposed in [3]. As shown in [9], the two singular values of $\mathbf{V}_k-\mathbf{V}_l$ are identical for such constellations. Thus, a_m, b_m in (19) and $d_m=\sigma_m\left(\mathbf{\Phi}_k^H\mathbf{\Phi}_l\right)$ no longer depend on m. After dropping the subscript m in a_m, b_m, and d_m, we can then write probability density function of $\frac{|\beta|}{\alpha+|\beta|}(Z_k-Z_l)$ as

$$f(x) = \frac{e^{-\frac{x}{2\alpha}-f_1}}{b}\sum_{n=0}^{\infty}\sum_{i=1}^{2N+n}\Big[g_{n,i,1}\frac{(-x/b)^{i-1}}{(i-1)!}e^{ax}u(-x) +g_{n,i,2}\frac{(x/b)^{i-1}}{(i-1)!}e^{-ax}u(x)\Big] \quad (26)$$

where $\widetilde{f}_1=f_1-\frac{f_2}{2\alpha}$, $\widetilde{f}_2=\frac{f_2}{b}$ and

$$g_{n,i,1}=\frac{(\widetilde{f}_1+\widetilde{f}_2ab)^n}{\Gamma(2N+n)(2ab)^{4N+2n-i}}\sum_{j=0}^{\min(n,2N+n-i)}\frac{(-1)^j}{j!(n-j)!} \times\frac{\Gamma(4N+2n-i-j)}{\Gamma(2N+n-i-j+1)}\left(\frac{\widetilde{f}_1}{2ab\widetilde{f}_2}+\frac{1}{2}\right)^{-j}, \quad (27)$$

$$g_{n,j,2}=\frac{(\widetilde{f}_1-\widetilde{f}_2ab)^n}{\Gamma(2N+n)(2ab)^{4N+2n-i}}\sum_{j=0}^{\min(n,2N+n-i)}\frac{1}{j!(n-j)!} \frac{\Gamma(4N+2n-i-j)}{\Gamma(2N+n-i-j+1)}\left(\frac{\widetilde{f}_1}{2ab\widetilde{f}_2}-\frac{1}{2}\right)^{-j}, \quad (28)$$

$$f_1 = \frac{\alpha+|\beta|}{\alpha|\beta|(1-d^2)}\Big[\frac{\alpha+|\beta|d^2}{\alpha+|\beta|}\left\|\overline{\mathbf{Y}}_1\right\|_F^2 +\left\|\overline{\mathbf{Y}}_2\right\|_F^2-2d\,\mathrm{Re}\,\mathrm{tr}\left(\overline{\mathbf{Y}}_2^H\overline{\mathbf{Y}}_1\right)\Big],$$

$$f_2 = \frac{1}{\alpha}\Big[\frac{\left(\alpha^2-|\beta|^2d^2\right)}{\alpha+|\beta|}\left\|\overline{\mathbf{Y}}_1\right\|_F^2 -(\alpha+|\beta|)\left\|\overline{\mathbf{Y}}_2\right\|_F^2+2|\beta|d\,\mathrm{Re}\,\mathrm{tr}\left(\overline{\mathbf{Y}}_2^H\overline{\mathbf{Y}}_1\right)\Big].$$

The PEP is obtained by $\int_0^\infty f(x)\,dx$, that is,

$$P_e(k,l)=e^{-f_1}\sum_{n=0}^{\infty}\sum_{i=1}^{2N+n}g_{n,i,2}\left(ab+\frac{b}{2\alpha}\right)^{-i}. \quad (29)$$

VI. Numerical Results

In this section, numerical results are presented to illustrate the performance of the MLD, SDD, and PBD under different Rician channels. The number of antennas is set to $M=N=2$. The diffuse fading component $\left\{\widetilde{\mathbf{H}}_\tau\right\}$ is generated by Jakes' model with no spatial correlation and identical time-correlation coefficients $\varphi_{h,\xi}=J_0(2\pi f_DT_s\xi)$ for $f_DT_s=0.05$ and $\xi=0,1,\ldots$. The time-varying LOS component is generated as in Section II with $\mu_{i,j}\in\mathbb{R}$ for $i,j=1,2$. The constellation proposed in [3] is used with the constellation size $L=16$.

In Fig.1, with $K=1$, $f_L=0.05$, $N=1$, the simulated symbol error probability (markers) are plotted against the analytic symbol error probabilities (curves), which are obtained from truncating the infinite sum in (29), averaging over all matrices in $\mathcal{S}$, and then applying the union bound. The averaging over the set $\mathcal{S}$ is necessary because the analytic results are conditioned on $\mathbf{S}_{\tau-1}$. Since $\varphi_{h,1} = J_0(2\pi \cdot 0.05) > 0$, the analytic results also apply for the SDD if the $\overline{\mathbf{X}}_\tau$ in (12) is used. Fig.1 shows good accuracy of the analytic results, which is expected because (29) is exact for the PEP.

To better understand the relative performance of the MLD, the PBD, and the SDD, they are simulated under different combinations of $f_L T_s$ and K values. In Fig.2, we fix $K = 1$ and plot the three demodulator under $f_L T_s = 0.03,\ 0.05$ respectively. Conversely, curves in Fig.3 are corresponding to a fixed Doppler shift $f_L T_s = 0.05$ and $K = 0.5,\ 5$. As we expected, the MLD performs best, the PBD the second, and the SDD the worst. Furthermore, the performance of all three demodulator degrade as the Doppler shift of the LOS increases or K increases. However, the MLD appears less sensitive to the increase in $f_L T_s$ than the SDD and PBD. When either K or $f_L T_s$ is small, performance of the PBD and the SDD are not far from the MLD's performance. Therefore, when the LOS component is either weak or nearly static, the simple SDD or PBD may be a good choice. On the other hand, when the LOS component is strong or fast varying, the PBD and the SDD are far from the optimal demodulation.

VII. Conclusion

Demodulation of DUSTM signals is studied in this paper for Rician fading channels. Analytic expressions and bounds on the PEP are derived for the MLD and SDD. The new results for Rician channel relate to performance metrics such as the effective SNR and diversity product which are well-studied in Rayleigh fading. These analytic results could be helpful towards a deeper understanding of the impact of various parameters in the Rician fading model. Additional results are obtained for the constellation in [3]. Unlike in the Rayleigh fading, the SDD and the PBD are usually not equivalent to the MLD. Performance of these demodulators are compared under different fading environments.

References

[1] B. M. Hochwald, W. Sweldens, "Differential unitary space-time modulation", *IEEE Trans. Comm.*, Dec. 2000

[2] B. M. Hochwald, T. L. Marzetta, "Unitary space-time modulation for multiple-antenna comuunications in Rayleigh flat fading", *IEEE Trans. Info. Theory*, Mar. 2000

[3] V. Tarokh, H. Jafarkhani, "A differential detection scheme for transmit diversity", *IEEE J. Sel. Areas in Comm.*, July 2000

[4] E. Chiavaccini, G. M. Vitetta, "Further results on differential space-time modulation", *IEEE Trans. Comm.*, July 2003

[5] C. B. Peel, A. L. Swindlehurst, "Effective SNR for space-time modulation over a time-varying Rician channel", *IEEE Trans. Info. Theory*, Jan. 2004

[6] C. B. Peel, A. L. Swindlehurst, "Performance of space-time modulation for a generalized time-varying Rician channel model", *IEEE Trans. Wireless Comm.*, May 2004

[7] R. Schober, L. H.-J. Lampe, "Bit-interleaved coded differential space-time modulation", *IEEE Trans. Comm.*, Sept. 2002

[8] T. Cui, C. Tellambura, "Multiple-symbol differential detection for single-antenna and multiple-antenna systems over Ricean-fading channels," *Proc. of ICC*, 2006

[9] H. Sui, J. R. Zeidler, "An explicit and unified error probability analysis of two detection schemes for differential unitary space-time modulation", *Proc. of the 39th Asilomar Conf.*, Nov. 2005

[10] G. L. Turin, "The characteristic function of Hermitian quadratic forms in complex normal variables", *Biometrika*, Vol.47, No.1/2, pp.199-201, Jun. 1960

[11] S. B. Provost, E. M. Rudiuk, "The exact distribution of indefinite quadratic forms in noncentral normal vectors", *Ann. Inst. Statist. Math.*, Vol.48, No.2, pp.381-394, 1996

[12] D. Raphaeli, "Distribution of noncentral indefinite quadratic forms in complex normal variables", *IEEE Trans. Info. Theory*, May 1996

[13] J. Cheng, T. Berger, "On the difference of two sums of independent generalized Gamma random variables with applications to error performance analysis and outage probability evaluation", *Proc. of IEEE Int. Symp. on Info. Theory (ISIT)*, July 2003

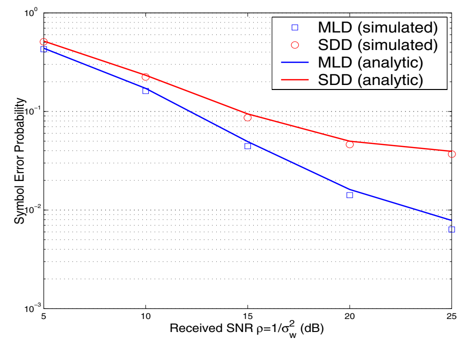

Fig. 1. Analytic versus simulated symbol error probability (K=1)

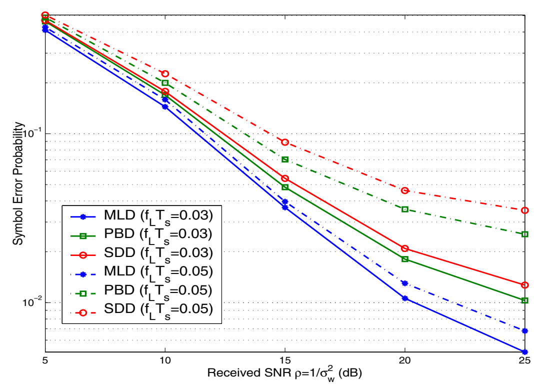

Fig. 2. Performance of the MLD, PBD, SDD: K=1, $f_L T_s$ = 0.03,0.05

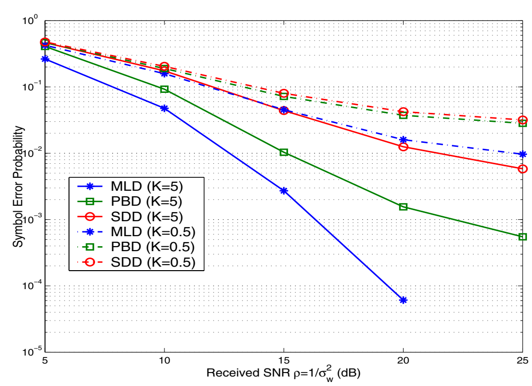

Fig. 3. Performance of the MLD, PBD, SDD: $f_L T_s$ = 0.05, K=0.5,5